

# IMPEDANCE-BASED TRANSPARENCY ANALYSIS OF HAPTIC TELEPRESENCE SYSTEMS

*Martin Kuschel, Martin Buss*

Technische Universität München  
Institute of Automatic Control Engineering (LSR)  
D-80290 Munich, Germany

## ABSTRACT

This paper provides a performance analysis of haptic (force-reflecting) telepresence systems. It is discussed how the mechanical properties displayed to the human operator are distorted from the mechanical properties of the remote environment. Reasons for distortions are communication delay and dynamics in the teleoperator and human-system interface. This work is related to earlier publications in our group [1–3] analysing the distortion of transparency by communication delay. Novel aspects herein are the additional consideration of robot dynamics. Experimental results illustrate the analysis.

## 1. INTRODUCTION

A telepresence system enables a human operator to perceive and manipulate a remote environment. The human operator handles the human system interface (HSI) to command the robotic teleoperator (TO) performing actions in a remote environment. HSI and TO exchange command and sensor feedback signals over a communication network (COM) such as the internet. To facilitate a high degree of immersion in telepresence, multiple modalities of human perception are addressed including visual, auditory, and haptic senses, see Fig. 1 for an illustration. An overview is given in [4]. Example applications for telepresence are tele-surgery, tele-assembly and tele-rescue systems, etc.

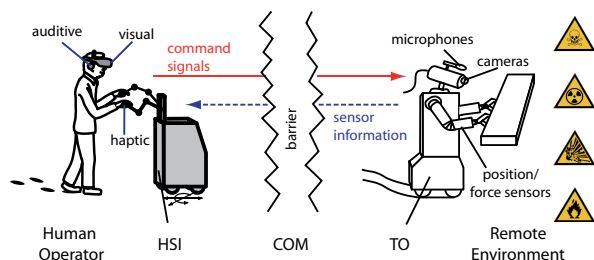


**Fig. 1.** Multimodal telepresence system.

This work is supported in part by German Research Foundation (DFG) within the collaborative research center SFB453 "High-Fidelity Telepresence and Teleaction". The authors appreciate contributions by students Uwe Friedrich and Luciano Valente.

The focus of this paper is on kinesthetic-haptic telepresence systems. Kinesthetic haptic (by now "haptic") perception involves perception of positions, forces, motions of joints, and muscles [5]. By haptic command and feedback signals energy is exchanged between HSI and TO. Thereby, a global control loop is closed via the COM. Main objectives in control system design are stability and transparency (remote environment should be identically reproduced by the HSI). Key challenges associated with these conflicting goals are communication delay and dynamics of the involved robots (HSI and TO).

While performance analyses of the haptic interface are reported in numerous publications, e.g. [6–9], principle performance analyses of the overall telepresence system have yielded only few practical results. In [10] basic concepts are defined based on the equality of the mechanical properties on remote and operator side. In [11] an analysis for soft environments is conducted. The impact of communication delay was recently investigated in [3, 12].

The paper provides a performance analysis of haptic telepresence systems in terms of transparency which is based on a comparison between the mechanical properties of the displayed environment and the remote environment. Thereby, the mechanical properties are modeled by transfer functions between angular joint velocity and torque.

The remainder of this paper is organized as follows: In Section 2 a brief background is presented followed a detailed analysis in Section 3. Simulations and experiments are provided in Section 4 and 5.

## 2. BACKGROUND - TELEPRESENCE AND TRANSPARENCY

This section introduces basic concepts to model haptic telepresence systems and the formal definition of transparency.

### 2.1. The Telepresence System

The basic structure of a haptic telepresence system with velocity-force architecture is shown in Fig. 2.

### 2.1.1. The HSI driven by the human operator

Consider the HSI as mechanical robot having an open kinematic chain of  $N$  rigid links, interconnected by  $N$  joints. The joints are actuated by electrical motors and assumed to be stiff. Let the vector  $\omega_h \in \mathbb{R}^N$  contain the angular link velocities and  $\tau_h \in \mathbb{R}^N$  the torques at the HSI. Further simplifications are: The motors and gears are modeled as uniform bodies having their center of mass on the rotation axis and ideal response. Force and velocity sensors have ideal responses. The dynamical model of the HSI attached to the human operator is

$$M_h \dot{\omega}_h + n_h = g_h - \tau_o. \quad (1)$$

Where  $M_h$  is the inertia matrix of the HSI and  $n_h$  comprises torques based on coriolis force, gravity, and friction. The vector  $g_h \in \mathbb{R}^N$  contains the motor torques of the HSI. The vector  $\tau_o$  contains the torques applied by the human operator measured by sensors attached to every link.

Input-output-linearization (computed torque method) according to [13] is conducted by commanding a torque depending on the reference acceleration  $\dot{\omega}_{h,\text{ref}}$

$$g_h = M_h M_1^{-1} \dot{\omega}_{h,\text{ref}} + n_h + \tau_o. \quad (2)$$

The virtual inertia matrix  $M_1$  renders the HSI to the masses  $M_1 = \text{diag}(M_{1,1}, M_{1,2}, \dots, M_{1,N})$ . The resulting dynamics are then described by

$$\dot{\omega}_h = M_1^{-1} \dot{\omega}_{h,\text{ref}}. \quad (3)$$

Torque control assures the realization of the reflected torque  $\tau_h$  upon the virtually rendered HSI. A controller

$C_1 : U \rightarrow M$  relates the torque difference to the reference acceleration

$$\dot{\omega}_{h,\text{ref}} = C_1(\tau_c - \tau_h). \quad (4)$$

Where the torques measured at the HSI depend on the human operator's dynamics,  $Z_o : U \rightarrow M$ , according to

$$\tau_h = Z_o(\omega_h). \quad (5)$$

Finally, the dynamics of the HSI driven by the human operator result in:

$$M_1 \dot{\omega}_h = C_1(\tau_c - Z_o(\omega_h)). \quad (6)$$

### 2.1.2. The COM

Exchanged command and feedback signals afflicted with communication delay can lead to instability of the overall system [14]. Therefore, the passivity paradigm is applied to stabilize the COM. A passive system does not generate energy. By definition an observable single-input-single-output system with zero initially stored energy is passive, if

$$\int_0^t p_{\text{in}}(\tau) d\tau \geq 0, \quad \forall t \geq 0. \quad (7)$$

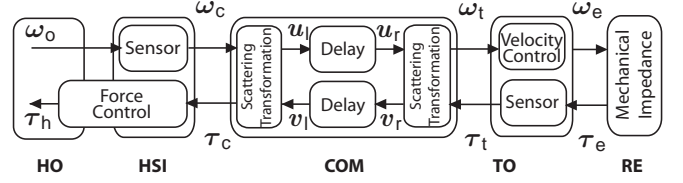


**Fig. 2.** Compensated haptic telepresence system in velocity-force architecture (HO - human operator, RE - remote environment)

Where  $p_{\text{in}}$  represents the instantaneous power input. Power is defined as scalar product of effort (torque  $\tau$ ) and flow (angular velocity  $\omega$ ) variables and

$$p_{\text{in}} = \omega_c \cdot \tau_c - \omega_t \cdot \tau_t. \quad (8)$$

is the power entering the COM-two-port. (The dot indicates the element-wise product;  $[\omega_c, \tau_c, \omega_t, \tau_t] \in \mathbb{R}^{4N}$  contain the scalar elements representing the single, corresponding links of HSI and TO).

In case of constant communication delays, the active COM can be passivated by the scattering transformation introduced in [14, 15]. The bijective transformation of effort and flow variables into scattering variables is given by

$$\begin{aligned} u_l &= \frac{b\omega_c + \tau_c}{\sqrt{2b}}, & v_l &= \frac{b\omega_c - \tau_c}{\sqrt{2b}}, \\ u_r &= \frac{b\omega_t + \tau_t}{\sqrt{2b}}, & v_r &= \frac{b\omega_t - \tau_t}{\sqrt{2b}}. \end{aligned} \quad (9)$$

Where  $u \in \mathbb{R}^N$  is the vector of the incident waves and  $v \in \mathbb{R}^N$  is the vector of the reflected waves. The parameter  $b > 0$  represents the wave impedance. The passive dynamics of the COM disturbed by a constant delay  $T_d$  are then given by

$$\begin{aligned} u_r(t) &= u_l(t - T_d), \\ v_l(t) &= v_r(t - T_d). \end{aligned} \quad (10)$$

### 2.1.3. The TO working in the remote environment

Consider a mechanical robot in configuration of the HSI. Consequently, the dynamical equation is given by

$$M_t \dot{\omega}_e + n_t = g_t - \tau_e \quad (11)$$

Where  $M_t$  and  $n_t$  denote again inertias and nonlinearities of the robot.  $g_t$  and  $\tau_e$  denote motor torques and external torques, respectively. Input-output linearization [13] is achieved by commanding

$$g_t = M_t M_2^{-1} \dot{\omega}_{e,\text{ref}} + n_t + \tau_e, \quad (12)$$

The resulting linear, decoupled dynamics,

$$\dot{\omega}_e = M_2^{-1} \dot{\omega}_{e,\text{ref}}, \quad (13)$$

render the robot links to the virtual mass  $M_1 = \text{diag}(M_{2,1}, M_{2,2}, \dots, M_{2,N})$ . A velocity controller,  $C_2 : U \rightarrow M$ , realizes the command signal  $\omega_t$

$$\dot{\omega}_{e,\text{ref}} = C_2(\omega_t - \omega_e). \quad (14)$$

The velocity-controlled TO is serially connected to the remote environment described by  $Z_e : U \rightarrow M$ . The resulting compensated system is finally described by

$$\begin{aligned} M_2 \dot{\omega}_e &= C_2(\omega_t - \omega_e), \\ \tau_t &= Z_e(\omega_e). \end{aligned} \quad (15)$$

## 2.2. Performance Evaluation by Transparency

Design goal of telepresence systems is the reproduction of the remote environment such that it enables the human operator at least to be "objectively present in the remote environment that is physically separate from the person in space" [16]. Means to measure objective telepresence in multimodal telepresence systems are e.g. task completion time or reaction time. Additionally, for haptic telepresence systems, the notion of ideal responses or transparency can be applied. According to [17] ideal transparency is defined as

$$Z_h(s) = Z_e(s). \quad (16)$$

This equation states that the displayed mechanical impedance  $Z_h$  should equal the mechanical impedance of the remote environment  $Z_e$  for ideal reproduction. Herein, impedances represent the properties of a system in frequency domain being the quotient between effort and flow variables (e.g. torque and angular velocity),  $Z(s) = \tau(s)/\omega(s)$ ;  $s$  denotes the complex frequency, respectively.

According to [18], the ideal response is the equality of position (angle) and force (torque) at operator and teleoperator side

$$\int_0^t \omega_h(\tau) d\tau = \int_0^t \omega_e(\tau) d\tau \quad \text{and} \quad \tau_h(t) = \tau_e(t). \quad (17)$$

It is equivalent to ideal transparency according to equation (16). Measure to evaluate transparency are obtained by integrating quadratic position and force errors

$$T_p = \int_0^{t_f} (\alpha_h - \alpha_e)^2 dt, \quad T_\tau = \int_0^{t_f} (\tau_h - \tau_e)^2 dt. \quad (18)$$

Where  $t_f$  is the final time of the teleoperation.

## 3. TRANSPARENCY ANALYSIS

The transparency analysis conducted here is based on the comparison between the displayed impedance and the impedance of the remote environment according to the transparency definition (16).

For sake of clarity the analysis is constraint to one robot link,  $N = 1$ . Telepresence system and subsystems are modeled as linear, time invariant systems based on the structure described in Section 2.1. They are denoted as transfer functions in complex frequency domain.

### 3.1. Displayed Impedance

The impedance of the remote environment as displayed to the human operator is

$$Z_h(s) = \frac{\tau_h(s)}{\omega_o(s)}. \quad (19)$$

The displayed impedance contains the dynamics of the torque-controlled HSI, the time-delayed COM and the velocity-controlled TO. According to Fig. 2 and it becomes

$$Z_h(s) = G_\tau(s) \frac{\tau_c(s)}{\omega_c(s)} = G_\tau(s) Z_c(s). \quad (20)$$

Where  $G_\tau$  denotes the transfer function of the torque-controlled HSI. Assuming a PID-control, equation (4) and (5) yield the transfer function

$$G_\tau(s) = \frac{C_1(s) Z_o(s)}{s M_1 + C_1(s) Z_o(s)} \quad (21)$$

$Z_c$  is defined by the dynamics of the COM two-port, equation (10), terminated by the impedance of the TO,  $Z_t$ . This leads to

$$Z_c(s) = b - 2b \frac{e^{-2T_d s} (b - Z_t)}{b + Z_t + e^{-2T_d s} (b - Z_t)} \quad (22)$$

in case of a constant-delayed communication by  $T_d$  (See also [1] for a detailed derivation.).  $Z_t$  is defined according to equation (15)

$$Z_t(s) = \frac{\tau_t(s)}{\omega_t(s)} = G_\omega(s) Z_e(s). \quad (23)$$

Where  $G_\omega$  denotes the velocity-controlled TO and  $Z_e$  the impedance of the remote environment. Assuming again a PID velocity controller, equation (14) results in the transfer function

$$G_\omega(s) = \frac{C_2(s)}{s M_2 + C_2(s)}. \quad (24)$$

### 3.2. Analysis

$Z_e$  denotes the impedance of the remote environment to be equal the displayed impedance in the ideal case. However, in reality the displayed impedance  $Z_o$  is spoiled by the dynamics of the HSI, the COM and the TO represented by the dynamics  $G_\tau(s)$ ,  $e^{-2sT_d}$ , and  $G_\omega(s)$ .

Investigating the border cases for the frequency  $s = 0$  and  $s \rightarrow \infty$  yields

$$Z_h(0) = Z_e(0), \quad \lim_{s \rightarrow \infty} Z_h(s) = 0 \quad (25)$$

if the control loops  $G_\tau$  and  $G_\omega$  exhibit static accuracy. Hence, ideal transparency according to equation (16) will be achieved in static state and relatively good transparency can be assumed for low frequencies.

In case the COM is terminated with an impedance matched to the wave impedance  $b$ , i.e.  $Z_t = b$ , the displayed impedance becomes

$$Z_h(s) \Big|_{Z_t=b} = bG_\tau(s). \quad (26)$$

This means, in case the TO reflects a damping behavior the displayed dynamics will nevertheless be spoiled by the dynamics of the HSI. Hence, transparency cannot be obtained by impedance matching (This statement was already obtained in [1] regarding only time delays.)

In case of instantaneous telepresence,  $T_d = 0$ , the displayed impedance becomes

$$Z_h(s) \Big|_{T_d=0} = G_\tau(s)G_\omega(s)Z_e(s). \quad (27)$$

This indicates that in case the COM does not induce retardation the capability of the telepresence system to reproduce the remote environment will still be decreased by the dynamics of HSI and TO. Good performance will be achieved for frequencies lower than the cut-off frequencies of the controlled robots.

An approximation of the communication delay by a 1st-order Padé element,

$$e^{-2T_d s} \approx \frac{1 - T_d s}{1 + T_d s}, \quad \forall \omega < \frac{1}{3T} \quad (28)$$

yields further insights. In case the teleoperator works in a free space environment the remote environment becomes  $Z_e = 0$  and according to equation (23),  $Z_t = 0$ . Consequently, the displayed impedance of free space is

$$Z_h^{\text{app}}(s) \Big|_{Z_t=0} = G_\tau(s)bT_d s. \quad (29)$$

That means in free space the force-controlled HSI renders a mass that is proportional to the wave impedance  $b$  and the communication delay  $T_d$ . Furthermore, a stiff wall ( $Z_e = k_i/s$ , with  $k \rightarrow \infty$ ) will be displayed as

$$Z_h^{\text{app}}(s) \Big|_{Z_e \rightarrow \infty} = G_\tau(s) \frac{b}{T_d s}. \quad (30)$$

That means a stiff wall is rendered by the force-controlled HSI as a compliant wall having a stiffness proportional to  $b$  but inversely proportional to  $T_d$ .

For a more specified analysis consider proportional control by  $C_1(s) = c_1$ , with  $c_1 = \text{const.} \in \mathbb{R}^+$  and a damping human operator,  $Z_o = \text{const.} \in \mathbb{R}^+$ ; then equation (21) yields the first order lag element

$$G_\tau(s) = \frac{1}{s \frac{M_1}{c_1 Z_o} + 1} \quad (31)$$

having a time constant  $T_1 = \frac{M_1}{c_1 Z_o}$ . Assuming a proportional velocity controller,  $C_2(s) = c_2$ , with  $c_2 = \text{const.} \in \mathbb{R}^+$ , equation (24) yields the first order lag element

$$G_\omega(s) = \frac{1}{s \frac{M_2}{c_2} + 1} \quad (32)$$

having a time constant  $T_2 = \frac{M_2}{c_2}$ . In this simplified case the dynamics of HSI, COM, and TO that prevent the telepresence system from achieving ideal transparency are represented by  $T_1$ ,  $T_d$ , and  $T_2$ . Equation (31) states that the time constant of the HSI proportionally depends on the relation between the mass of the HSI and the control gain but is anti-proportional to the impedance of the human operator. That means, the mass of the HSI is partly compensated by the damping of the operator. On the other hand, the time constant of the TO,  $T_2$ , proportionally depends on the relation between mass and control gain.

#### 4. SIMULATIONS

Amplitude responses were computed using Matlab/ Simulink. The impedance of the operator was  $Z_o = 10$  (damper). Communication delay was approximated by a 1st-order Padé approximation. The first plot (Fig. 3) shows the telepresence system rendering a mass  $Z_e = 10s$ . The upper diagram shows the impact of different communication delays. Time constants of the robots were held nearly ideal at  $T_1 = T_2 = 0.05$  s. While transparency is obtained for low frequencies

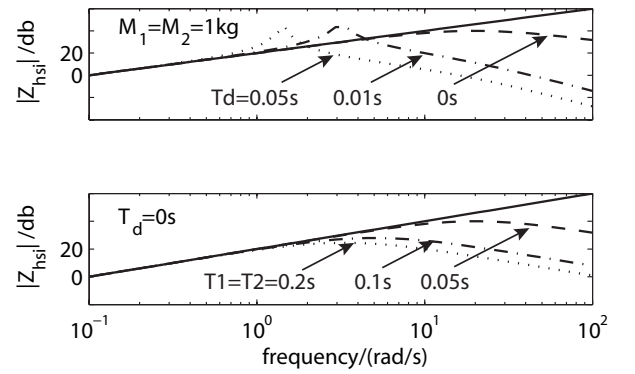


**Fig. 3.** Amplitude response of displayed impedance compared and remote environment (solid line). Mass effects by communication delay and compliance effects by HSI and TO spoil transparency.

mass-effects spoil performance. A similar result was obtained for moving in free space  $Z_e = 0$  in equation (29). Higher frequencies are spoiled by compliance-effects. The lower diagram depicts the influence of robot dynamics (HSI and TO). Communication delay was set to zero,  $T_d = 0$ . As stated in equation (25) good transparency is obtained for low frequencies smaller 2 rad/s. However, the low-pass characteristics of

the robots damp high frequencies and spoil telepresence, as stated in equations (25), (27). The higher the time constants and the communication delay the lower the transparency. The second plot (Fig. 4) shows the same simulation but with the remote environment being a compliant wall with a stiffness of  $Z_e = 10 \frac{1}{s}$ . The distortions by communication delay (upper diagram) are lower but the compliance effects caused by the dynamics of HSI and TO (lower diagram) are still valid.

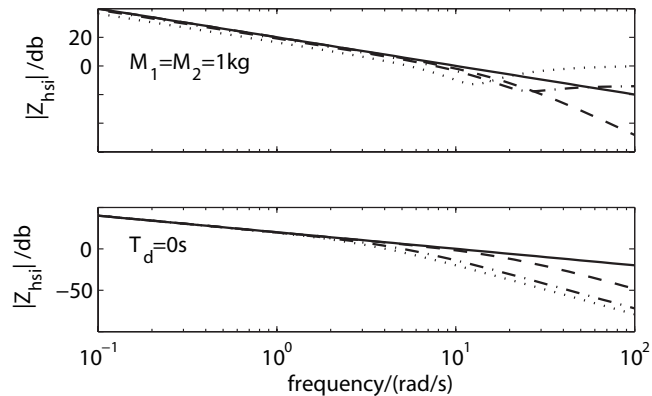


**Fig. 4.** Amplitude response of displayed and remote impedance (solid line). Compliance effects by HSI and TO spoil transparency.

## 5. EXPERIMENTS

An experimental evaluation was performed using a two degree-of-freedom haptic telepresence system. The setup is shown in Fig. 5. It consists of two identical SCARA-robots with two degrees of freedom connected to a PC. The link angles are measured by an incremental encoder, the torque applied to each link by strain gauges (calibrated during the first five seconds of each trial). The sensor data are processed in a PC

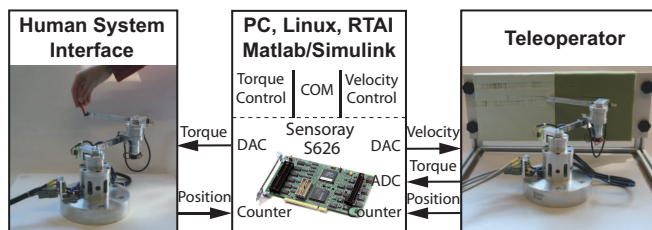


**Fig. 5.** Experimental 2-DoF haptic telepresence system.

running RTAI-RealTime Application Interface for Linux. All control algorithms (HSI torque control, TO velocity control in joint space) are implemented as Matlab/Simulink models with realtime code generated automatically. An input-output-linearization as described in Section 2.1 enabled the definition of virtual masses upon the SCARA-robots. The control loops operate at a sampling rate of 1000 Hz. The controllers are proportional elements designed for low masses

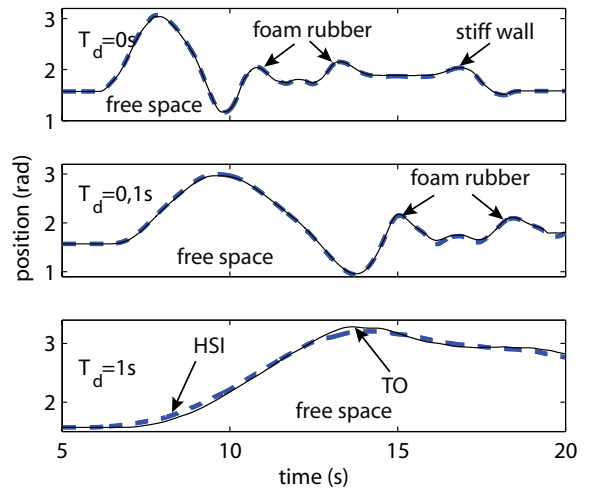


**Fig. 6.** Telepresence disturbed by communication delay: Stabilization efforts resulted in an increase of task completion time. (HSI - dashed line, TO - solid line)

( $M_1 = M_2 = 10$  kg). The performed trajectory consisted of moving in free space, compliant environment (foam rubber) and stiff environment. This provides a trajectory as depicted in the first diagram of Fig 6. The successive figures show the impact of passivated communication delay to the positioning of the HSI (dashed line) and TO (solid line) (Virtual masses are set to  $M_1 = M_2 = 1$  kg). The induced mass effects proportionally to the communication delay result in an increase of task completion time. The operator was not able to complete the demanded trajectory. Position deviations in the last diagram illustrate the concurrent decrease of stiffness.

The impact of different dynamics of HSI and TO on the

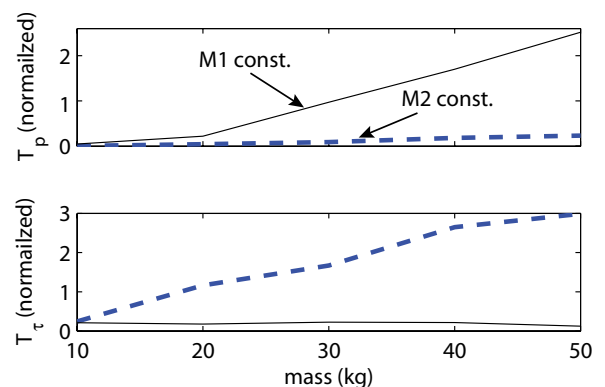


**Fig. 7.** Transparency of the telepresence system disturbed by dynamics of HSI and TO. Position deviation is caused by a heavy TO (solid line). Torque deviation is caused by a heavy HSI (dashed line).

transparency according to equations (18) is shown in Fig. 7. Communication delay was set to zero and mass of HSI and TO were altered. Position deviation (upper diagram) is large

when the velocity controlled TO is heavy, i.e. when  $M_2$  increases. Torque deviation (lower diagram) is large when the mass of the HSI,  $M_1$ , increases. In this case, the operator is not able to react quickly upon the reflected torque driving the TO further into the remote environment.

## 6. CONCLUSION

In this work an impedance-based transparency analysis for haptic telepresence systems in velocity-torque architecture was conducted. To illustrate the impact of the involved robots, a linearized, decoupled and compensated haptic telepresence systems was set up theoretically and in real. The displayed impedance by the HSI was analyzed. It can be stated that ideal transparency is achieved in static state and good performance can be assumed for very low communication delays and in case of frequencies lower than the cut-off frequencies of HSI and TO. The model should be extended to an active operator closing the loop between reflected torque and commanded velocity. Furthermore, transparency should to be analyzed when the different distortions occur concurrently.

## 7. REFERENCES

- [1] Martin Kuschel, Sandra Hirche, and Martin Buss, "Communication-induced disturbances in haptic telepresence systems," in *Proceedings of the International Federation of Automatic Control*, Prague, Czech Republic, 2005.
- [2] Sandra Hirche, Andrea Bauer, and Martin Buss, "Transparency of haptic telepresence with constant time delay," in *IEEE Conference on Control and Applications*, Toronto, Canada, 2005, pp. 328–333.
- [3] Sandra Hirche, *Haptic Telepresence in Packet Switched Communication Networks*, Ph.D. thesis, Technische Universität München, 2005.
- [4] Thoma B. Sheridan, "Musings on telepresence and virtual telepresence," *Presence*, vol. 1, pp. pp.120–125, 1992.
- [5] E. Bruce Goldstein, *Sensation and Perception*, Wadsworth Publishing, 6th edition, 2002.
- [6] J. Edward Colgate and J. Michael Brown, "Factors affecting the z-width of a haptic display," in *Proceedings of the International Conference on Robotics and Automation*. 1994, pp. 3205–3210, IEEE.
- [7] Vincent Hayward and Oliver R. Astley, "Performance measures for haptic interfaces," *Robotics Research*, vol. -, pp. 195–207, 1996.
- [8] Dale A. Lawrence, Lucy Y. Pao, Anne M. Dougherty, Mark A. Salada, and Yiannis Pavlou, "Rate-hardness: A new performance metric for haptic interfaces," *IEEE Transactions on Robotics and Automation*, vol. 16, no. 4, pp. 357–371, 2000.
- [9] Yoshiyuki Tanaka, Toshio Tsuji, and Hideki Miyaguchi, "Analysis of human perception for robot impedance," in *Proceedings of the International Federation of Automatic Control*, Prague, Czech Republic, 2005.
- [10] Blake Hannaford, "A design framework for teleoperators with kinesthetic feedback," in *IEEE Trans. Robotics and Automation*, 1989, vol. 5, pp. 426–434.
- [11] Murat Cenk Cavosoglu, Alana Sherman, and Frank Tendick, "Design of bilateral teleoperation controllers for haptic exploration and telemanipulation of soft environments," *Proceedings of the IEEE International Conference on Robotics and Automation*, vol. 18, pp. 641–647, 2002.
- [12] Neil A. Tanner and Günther Niemeyer, "Improving perception in time-delayed telerobotics," *International Journal of Robotics Research*, vol. 24, no. 8, pp. 631–644, 2005.
- [13] Lorenzo Sciavicco and Bruno Siciliano, *Modelling and Control of Robot Manipulators*, Springer, 1 edition, 2003.
- [14] Robert J. Anderson and Mark W. Spong, "Bilateral control of teleoperators with time delay," in *Proceedings of the IEEE International Conference on Robotics and Automation*, 1989, pp. vol.34, pp. 494–501.
- [15] Günther Niemeyer, *Using Wave Variables in Time Delayed Force Reflecting Teleoperation*, Ph.D. thesis, MIT, Department of Aeronautics and Astronautics, September 1996.
- [16] David W. Schloerb, "A quantitative measure of telepresence," *Presence*, vol. 4, pp. 64–80, 1995.
- [17] Dale A. Lawrence, "Stability and transparency in bilateral teleoperation," *IEEE Transactions on Robotics and Automation*, vol. 9, pp. 624–637, 1993.
- [18] Yasuyoshi Yokokohji, "Bilateral control of master-slave manipulators for ideal kinesthetic coupling - formulation and experiment," *IEEE Transactions on Robotics and Automation*, vol. 10, pp. 605–620, 1994.